EXCITATION AND GROWTH RATE OF ELECTROHYDRODYNAMIC INSTABILITIES

by

JOSEPH MICHAEL CROWLEY

S.B., Massachusetts Institute of Technology
(1962)

SUBMITTED IN PARTIAL FULFILLMENT OF THE
REQUIREMENTS FOR THE DEGREE OF
MASTER OF SCIENCE

at the

MASSACHUSETTS INSTITUTE OF TECHNOLOGY
August, 1963

Signature of Author _____
Department of Electrical Engineering, August 19, 1963

Certified by _____
Thesis Supervisor

Accepted by _____
Chairman, Departmental Committee on Graduate Students

EXCITATION AND GROWTH RATE OF ELECTROHYDRODYNAMIC INSTABILITIES

by

JOSEPH MICHAEL CROWLEY

Submitted to the Department of Electrical Engineering on August 19, 1963 in partial fulfillment of the requirements for the degree of Master of Science.

ABSTRACT

Waves on a planar water jet are studied theoretically and experimentally. The effects of surface tension, viscosity, and an applied electric field are included in the analysis. It is found theoretically that for a thin jet of water, the influence of viscosity is slight, so that the jet may be considered practically non-viscous. This finding is experimentally verified for the growth rate of an unstable wave on a water jet.

A method of exciting waves on a liquid jet is also studied. The theoretical model predicts certain nulls in the frequency response curve which are experimentally observed. The theoretically predicted shape of the frequency response curve is also experimentally verified.

Thesis Supervisor: James R. Melcher
Title: Assistant Professor of Electrical Engineering

ACKNOWLEDGEMENT

The author would like to thank Professor James R. Melcher, both for suggesting this problem and for his constant help and guidance during the course of the work. Thanks are also due Miss Marguerite A. Daly for typing the thesis.

Part of the numerical work was performed at the M.I.T. Computation Center, Cambridge, Mass. This work was supported in part by the National Aeronautics and Space Administration, Research Grant NsG-368.

Table of Contents

LIST OF FIGURES

p Pressure

R Equilibrium radius of a circular jet

$S_k = \sinh \frac{k\Delta}{2}$

$S_m = \sinh \frac{m\Delta}{2}$

T Surface tension

T_{ij} The ij^{th} component of the Maxwell stress tensor

t Time

t_o The time that a differential length of the jet enters the exciter

V Velocity of capillary waves

V_o Equilibrium velocity of the jet

V_k Phase velocity of a surface wave

u_i A solution of the fluid equations for v_1

v_i Velocity in the x_i^{th} direction

$v_2' = \frac{mh^2 v_2}{2\varepsilon_o e_o \phi_o}$

x_i Distances in a Cartesian coordinate system

$y = \omega - k_2 V_o$

$\alpha = \frac{V_k x_1}{V_o \ell}$

Δ Thickness of the jet

$\Delta' = \frac{\rho V_o^2 \Delta}{T}$

$\delta = k - \frac{\omega}{V_o}$

$\delta' = \frac{\delta T}{\rho V_o^2}$

$\delta_{\alpha\beta}$ Kronecker delta function

$\delta(x)$ Dirac delta function

ε Permittivity

ε_o Permittivity of free space

θ_p Phase angle

κ Amplitude parameter

μ Dynamic viscosity

ν Kinematic viscosity

$\nu' = \frac{\nu \rho V_o}{T}$

$\xi' = \xi[(1 - \frac{V_k^2}{V_o^2}) \frac{2\varepsilon_o e_o \phi_o}{mh^2} \frac{\ell}{aV_o}]^{-1}$

ξ_s Position of s^{th} interface

$\pi = 3.14159...$

ρ_e Electric charge density

ρ Mass density

σ Electrical conductivity

$\bar{\bar{\tau}}$ Stress tensor

τ_t Discontinuity of stress due to surface tension

ϕ Electric potential

ϕ_{o1}, ϕ_{o2} The DC bias voltage on the exciter plates

ϕ_1, ϕ_2 The signal voltage on the exciter plates

ω Angular frequency

$$\omega' = \frac{\omega \ell}{V_o}$$

$$\omega^* = \frac{\omega T}{\rho V_o^3}$$

$$\omega_o^2 = \frac{Tk^3}{\rho} - \frac{\varepsilon E_o^2 k^2}{\rho} \coth kb$$

CHAPTER I

Introduction

Recently there has been a revival of interest in the dynamics of liquids stressed by an electric field. Melcher[1] and Hoppie[2] have studied waves and instabilities on the surface of stationary and moving fluids both experimentally and theoretically, and Lyon[3] has studied the EHD Kelvin-Helmholtz instability theoretically. However, none of these analyses have included the effect of losses in the system, so that no attempt was made to measure the rate of growth of the instabilities or the damping of the stable waves. In this thesis we will consider experimentally and theoretically the effect of viscosity on waves on a jet.

Chapter II treats waves on the surface of a liquid jet. The equations of the system are solved with the aid of the boundary conditions and the dispersion relation is derived. The solution of this equation is considered in the limits of a very thick and a very thin jet. The result shows that in the limit of a very thin jet, the effect of the viscosity on the waves becomes vanishingly small due to the large surface to volume ratio. The growth rate of waves on a jet is then studied experimentally, and compared to the theoretical results.

In previous work, EHD waves have been excited by both applied electric fields and mechanical vibrations. The lack of an adequate model for the exciter, however, made it impossible to relate the response of the system to the exciter input.

In Chapter III, a model of a surface wave exciter is analyzed, and the results are used to determine the magnitude

of waves excited on a jet. The model predicts nulls in the frequency response and in the spatial response of the jet. These are both observed experimentally. The frequency response of the exciter is also measured for low frequencies, and compared to the theoretical predictions.

In Appendix A we apply a technique suggested by Chandrasekhar to show that the state of marginal stability of the fluid is determined by setting

$$\omega = 0.$$

This result can then be used to show that the onset of instability is not influenced by viscosity.

CHAPTER II

Waves on a Jet

2.0 Introduction

We will consider a jet of fluid unbounded in the x_2 and x_3 directions which is moving with a velocity V_o in the x_2 direction. The thickness of the jet is Δ (Fig. 2.1). An electric field is applied which is normal to the undisturbed surface of the fluid, and waves are propagating along this surface. We shall assume that the fluid above and below the jet is perfectly insulating and weightless, which is very nearly the case with air and a conducting liquid. The heavy fluid is supposed to be a perfect conductor, or equivalently, to have an electric relaxation time which is very short compared to the period of the disturbance. This requirement is easily met, even for very poor conductors, since the relaxation time is of the order of ε/σ. This means that a fluid with the relatively low conductivity of 1 mho/meter has a relaxation time on the order of 10^{-11} seconds, far less than the typical wave period, which is on the order of 10^{-3} seconds. In addition, we will neglect the effect of the induced magnetic field in the interaction. (The interactions discussed are quasistatic in nature.) The forces which do play a part in this analysis are surface tension, the electric field, and viscosity.

The equations which will be used to describe the electric field are Maxwell's electric field equations

$$\nabla \times \bar{E} = 0 \tag{2.1}$$

$$\nabla \cdot \bar{E} = \rho_e/\varepsilon_o \tag{2.2}$$

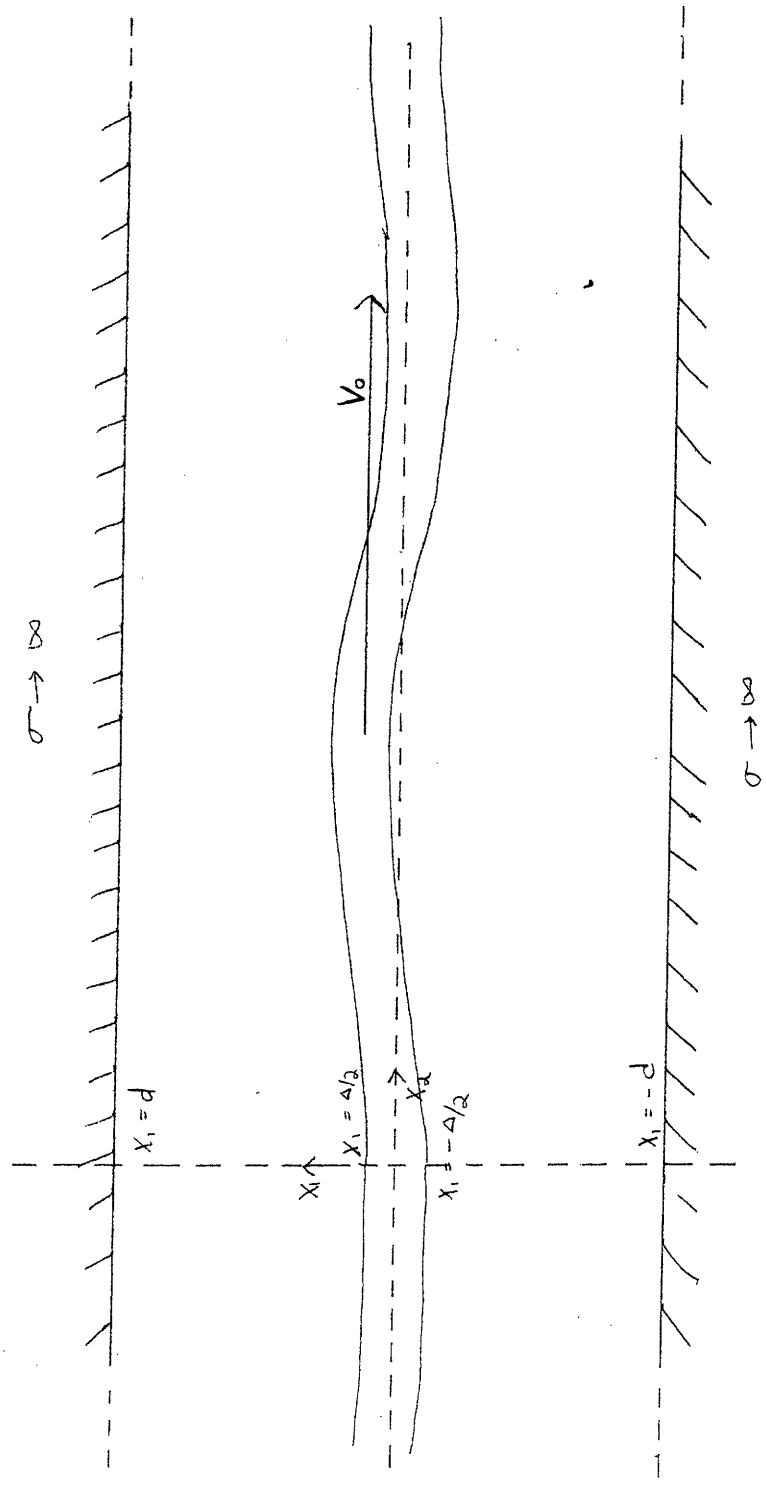

Figure 2.1 The EHD Jet

and their associated boundary conditions

$$\bar{n} \times [\![\bar{E}]\!] = 0 \tag{2.3}$$

$$\bar{n} \cdot [\![\varepsilon_o \bar{E}]\!] = \sigma_f \tag{2.4}$$

where $[\![\bar{E}]\!]$ represents the discontinuity in $\bar{E}$. The equations which describe the motion of the fluid are the Navier-Stokes equations and the continuity of mass equation

$$\rho \frac{d\bar{v}}{dt} = -\bar{\nabla}p + \mu\nabla^2\bar{v} = \bar{\nabla}\bar{\tau} \tag{2.5}$$

$$\bar{\nabla} \cdot \bar{v} = 0 \tag{2.6}$$

and their associated boundary conditions[5]

$$n_\alpha [\![\tau_{\alpha\beta}]\!] = T(\frac{1}{R_1} + \frac{1}{R_2}) \tag{2.7}$$

$$\bar{n} \cdot [\![\bar{v}]\!] = 0 \tag{2.8}$$

where $\tau_{\alpha\beta}$ is the stress tensor in the fluid, composed of pressure, viscous, and electric stresses, and $T(\frac{1}{R_1} + \frac{1}{R_2})$ represents the discontinuity of the stress attributed to the surface tension at the interface.

The electric and mechanical parts of the problem are coupled only at the interface, whose shape, which is determined in part by the electric field, determines the electric field. These equations are highly nonlinear, and cannot be solved as they stand. Therefore, we will use the technique of amplitude parameter expansion to obtain a series solution to these equations. To do this, we will expand all the unknowns in terms of an amplitude parameter κ, which we shall take to be the ratio of the wave amplitude to the wave length

$$f = f^0 + \kappa f^1 + \kappa^2 f^2 + \ldots$$

If the technique is successful, when we substitute these series into the equations, each power of κ will be the coefficient of a set of equations which can be solved in terms of the solutions of lower order equations. Then, each of the unknowns will be given by a series in the amplitude parameter. If the disturbance is very small, $\kappa f_1/f_o \ll 1$, the first two terms of the series will give a close approximation to the correct solution.

Physically, the zero-order terms represent the motion and fields which are not due to the surface waves, such as static equilibrium or rotation. In this investigation, it is assumed that the zero-order solution represents only a static equilibrium and the higher-order terms are all due to the wave motion of the surface. To the first order, this motion will be represented by a single eigenfunction, for instance, a sine wave in rectangular geometry, or a Bessel function in cylindrical geometry.

The potential at the boundary $x_1 = \pm d$ is fixed at the value $\phi = \phi_o$, and the potential at the surface of the conducting liquid is fixed at $\phi = 0$. Here the boundaries are equipotentials, but one of them, representing the surface of the liquid, may assume any shape. Since there are no simple solutions of Laplace's equation which will satisfy this type of boundary condition, we will assume a small sinusoidal disturbance of the liquid surface, and find the approximate electric field by a means of the amplitude parameter expansion.

2.1 Motion of the Jet

The motion of the fluid is governed by the Navier-Stokes equations for the motion of an incompressible, viscous fluid, and the equation of continuity, which are restated for convenience.

$$\rho[\frac{\partial \bar{v}}{\partial t} + \bar{v}\cdot\bar{\nabla}\bar{v}] = -\bar{\nabla}p + \mu\nabla^2\bar{v} \tag{2.9}$$

$$\bar{\nabla}\cdot\bar{v} = 0 \tag{2.10}$$

The amplitude parameter expansions for the pressure and velocity are

$$\bar{v} = \bar{V}_o + \kappa\bar{v} \tag{2.11}$$

$$p = \overset{0}{p} + \kappa\overset{1}{p} + \ldots \tag{2.12}$$

For the zero-order equations, we have

$$0 = -\nabla\overset{0}{p} \tag{2.13}$$

with the solution

$$\overset{0}{p} = \text{const.} \tag{2.14}$$

The first-order equations are

$$\rho[\frac{\partial}{\partial t}\bar{v} + (\bar{V}_o \cdot \bar{\nabla})\bar{v}] = -\bar{\nabla}p + \mu\nabla^2\bar{v} \tag{2.15}$$

$$\bar{\nabla}\cdot\bar{v} = 0 \tag{2.16}$$

We will assume that all first order quantities are waves propagating in the x_2x_3 plane, so that they may be written in the form

$$f(x_1,x_2,x_3,t) = \text{Re}[f(x_1)\exp i(k_2x_2 + k_3x_3 - \omega t)] \tag{2.17}$$

These basic solutions may be used to build up any arbitrary disturbance by means of Fourier techniques. Then the equations become

$$Dp = i\rho(\omega-k_2V_o)v_1 + \mu(D^2-k^2)v_1 \tag{2.18a}$$

$$ik_2p = i\rho(\omega-k_2V_o)v_2 + \mu(D^2-k^2)v_2 \tag{2.18b}$$

$$ik_3p = i\rho(\omega-k_2V_o)v_3 + \mu(D^2-k^2)v_3 \tag{2.18c}$$

$$Dv_1 + ik_2v_2 + ik_3v_3 = 0 \tag{2.19}$$

where

$$D = \frac{d}{dx_1}$$

Letting

$$y = \omega - k_2V_o \tag{2.20}$$

we find the solution

$$p = \frac{iy\rho}{k}[A \sinh kx_1 + B \cosh kx_1] \tag{2.21}$$

$$v_1 = A \cosh kx_1 + B \cosh kx_1 - \frac{i}{m}(k_2C + k_3F)\sinh mx_1 - \frac{i}{m}(k_2K + k_3G)\cosh mx_1 \tag{2.22a}$$

$$v_2 = \frac{ik_2}{k}(A \sinh kx_1 + B \cosh kx_1) + C \cosh mx_1 + K \sinh mx_1 \tag{2.22b}$$

$$v_3 = \frac{ik_3}{k}(A \sinh kx_1 + B \cosh kx_1) + F \cosh mx_1 + G \sinh mx_1 \tag{2.22c}$$

with

$$m^2 = k^2 - \frac{iy}{\nu} \tag{2.23}$$

A, B, C, F, and G, and K are constants whose values are determined from the boundary conditions.

The interfaces can be defined by the equation

$$\bar{F} = x_1 \mp \frac{\Delta}{2} - \xi(x_2,x_3,t) = 0 \tag{2.24}$$

where ξ is the displacement of the surface from the static equilibrium. Then we have, from the definition of the interface,

$$\frac{dF}{dt} = \frac{\partial F}{\partial t} + (\bar{v}\cdot\bar{\nabla})F = 0 \tag{2.25}$$

and from the definition of the normal vector

$$\bar{n} = \frac{\bar{\nabla}F}{|\bar{\nabla}F|} \tag{2.26}$$

Writing ξ in the amplitude parameter expansion we obtain

$$\bar{n} = \bar{a}_1 - \frac{\partial \xi}{\partial x_2}\bar{a}_2 - \frac{\partial \xi}{\partial x_3}\bar{a}_3 \tag{2.27}$$

$$v_1 = \frac{\partial \xi}{\partial t} \tag{2.28}$$

to the first order in κ. Now the position of the interface is defined in terms of the velocity of the fluid at the interface position. Since we have assumed that ξ has the same wave-like dependence as the other quantities in the problem we obtain

$$\xi = -\frac{1}{i\omega}v_1 = -\frac{A}{i\omega}\exp(kx_1) + \frac{1}{m\omega}(k_2B + k_3C)\exp(mx_1) \tag{2.29}$$

2.2 The Electric Field

Now we are in a position to determine the electric field. The amplitude parameter expansion takes the form

$$E_1 = E_o + \kappa e_1 \tag{2.30a}$$

$$E_2 = \kappa e_2 \tag{2.30b}$$

$$E_3 = \kappa e_3 \tag{2.30c}$$

where E_o is given by

$$E_o = \frac{\phi_o}{b} \tag{2.31}$$

The first order equations are

$$\bar{\nabla} \cdot \bar{e} = 0 \tag{2.32}$$

$$\bar{\nabla} \times \bar{e} = 0 \tag{2.33}$$

Now, making the assumption of waves in the x_2x_3 plane, we get the equations

$$De_1 + ik_2e_2 + ik_3e_3 = 0 \tag{2.34}$$

$$ik_2e_1 = De_2 \tag{2.35a}$$

$$ik_3e_1 = De_3 \tag{2.35b}$$

$$ik_3e_2 = ik_2e_3 \tag{2.35c}$$

The components of the normal are, to the first order,

$$n_1 = 1 \tag{2.36a}$$

$$n_2 = -ik_2\xi \tag{2.36b}$$

$$n_3 = -ik_3\xi \tag{2.36c}$$

where we have again made the assumption of periodic waves in the x_2x_3 plane. Then, using the boundary conditions

$$\bar{n} \times \bar{E} = 0 \quad \text{at } x_1 = \xi + \Delta/2 \tag{2.37}$$

$$e_2 = e_3 = 0 \quad \text{at} \quad x_1 = d \tag{2.38}$$

The solutions to the first order field equations are given by

$$e_1 = kE_o\xi \frac{\cosh k(d-x)}{\sinh kb} \tag{2.39a}$$

$$e_2 = -ik_2E_o\xi \frac{\sinh k(d-x)}{\sinh kb} \tag{2.39b}$$

$$e_3 = -ik_3E_o\xi \frac{\sinh k(d-x)}{\sinh kb} \tag{2.39c}$$

The electric field at the interface $x_1 = \xi + \Delta/2$ follows from these results.

$$E_1 = E_o + kE_o\xi \coth kb \tag{2.40a}$$

$$E_2 = -ik_2E_o\xi \tag{2.40b}$$

$$E_3 = -ik_3E_o\xi \tag{2.40c}$$

where

$$b = d - \Delta/2$$

Similarly, the electric field at the interface $x_1 = \xi - \Delta/2$ is given by

$$E_1 = E_o - kE_o\xi \coth kb \tag{2.41a}$$

$$E_2 = ik_2E_o\xi \tag{2.41b}$$

$$E_3 = ik_3E_o\xi \tag{2.41c}$$

2.3 The Dispersion Relation

We must still satisfy the boundary condition requiring continuity of the stress tensor at the fluid surface, which to the first order may be stated

$$n_\beta[\mp p\ \delta_{\alpha\beta} \pm \mu(\frac{\partial v_\alpha}{\partial x_\beta} + \frac{\partial v_\beta}{\partial x_\alpha}) \mp T_{ij} - T(\frac{\partial^2}{\partial x_2^2} + \frac{\partial^2}{\partial x_3^2})\xi^{\pm} \delta_{\alpha\beta}] = 0 \tag{2.42}$$

The quantities in this equation may be obtained from the solutions of the mechanical and electrical equations of the system, and the definition of the normal. Then the first order equations become

$$[(y^2 + 2i\nu k^2 y)S_k - \omega_o^2 C_k]A \pm [(y^2 + 2i\nu k^2 y)C_k - \omega_o^2 S_k]B$$

$$\pm [2\nu k k_2 y C_m + \frac{ik_2}{m}\omega_o^2 S_m]C + [2\nu k k_2 y S_m + \frac{ik_2}{m}\omega_o^2 C_m]K$$

$$\pm [2\nu k k_3 y C_m + \frac{ik_3}{m}\omega_o^2 S_m]F + [2\nu k k_3 y S_m + \frac{ik_3}{m}\omega_o^2 C_m]G = 0 \tag{2.43a}$$

$$(2ik_2C_k)A \pm (2ik_2S_k)B \pm \frac{1}{m}(k_2^2 + m^2)S_mC$$

$$+ \frac{1}{m}(k_2^2 + m^2)C_mK \pm (\frac{k_2k_3}{m} S_m)F + (\frac{k_2k_3}{m} C_m)G = 0 \qquad (2.43b)$$

$$(2ik_3C_k)A \pm (2ik_3S_k)B \pm (\frac{k_2k_3}{m} S_m)C$$

$$+(\frac{k_2k_3}{m} C_m)K \pm \frac{1}{m}(k_3^2 + m^2)S_mF + \frac{1}{m}(k_3^2 + m^2)C_mG = 0 \qquad (2.43c)$$

for the upper and lower surfaces, respectively, with

$$C_k = \cosh \frac{k\Delta}{2} \qquad C_m = \cosh \frac{m\Delta}{2} \qquad (2.44a,b)$$

$$S_k = \sinh \frac{k\Delta}{2} \qquad S_m = \sinh \frac{m\Delta}{2} \qquad (2.44c,d)$$

and

$$\omega_o^2 = \frac{Tk^3}{\rho} - \frac{\varepsilon E_o^2 k^2}{\rho} \coth kb \qquad (2.45)$$

Looking at these two sets of equations, we see that the coefficients of A, D, and G are identical for the corresponding equations for the upper and lower surfaces, while the coefficients of B, C, and F are the same except for a change of sign. Thus, by adding and subtracting the two sets of equations, we find that the solution splits into two modes, the symmetric mode with the arbitrary constants B, C, and F in which the upper and lower surfaces move in opposite directions, and the anti-symmetric mode with arbitrary constants A, D, and G in which the two surfaces move together. This splitting of modes comes about because the forces in this situation (surface tension, viscosity, pressure and electric pressure) act always toward or always away from the jet regardless of the orientation of the surface on which they are acting. The inclusion of a force

which does not act like this, such as gravity, would not allow the modes to split. Let us now consider the antisymmetric mode.

A non-trivial solution of equations 2.43 is possible only if the determinant of the coefficients of the arbitrary constants vanishes. This condition yields the dispersion relation

$$\begin{vmatrix} (y^2+2i\nu k^2 y)S_k-\omega_o^2 C_k & \frac{ik_2}{m}(\omega_o^2 C_m-2i\nu kmyS_m) & \frac{ik_3}{m}(\omega_o^2 C_m-2i\nu kmyS_m) \\ 2ik_2 C_k & \frac{1}{m}(k_2^2+m^2)C_m & \frac{k_2k_3}{m}C_m \\ 2ik_3 C_k & \frac{k_2k_3}{m}C_m & \frac{1}{m}(k_3^2+m^2)C_m \end{vmatrix} = 0 \qquad (2.46)$$

This may be written

$$y^2(m^2+k^2)-\omega_o^2(m^2-k^2)\coth\frac{k\Delta}{2}+2i\nu k^2 y(k^2+m^2) -2mk\coth\frac{k\Delta}{2}\tanh\frac{m\Delta}{2}) = 0 \qquad (2.47)$$

At this point it is interesting to consider whether the inclusion of viscosity will affect the criterion for the onset of instability. Since the instability on the surface of the jet may be thought of as a stationary instability viewed in a moving reference frame, the criterion for instability should be identical to that for a stationary fluid (in the absence of boundaries which are not moving with a velocity different from that of the fluid). To determine the state of marginal stability of a stationary fluid, we must find the condition for which the imaginary part of ω first becomes greater than zero, so that the disturbance neither grows nor dies. In the non-viscous case, the answer follows

easily, since the dispersion relation may be written

$$\omega = \pm \omega_o$$

where ω_o is either pure real or pure imaginary. If ω_o is real the imaginary part of ω must be zero, and if ω_o is imaginary, the real part of ω must be zero. Then the point at which the imaginary part of ω first becomes greater than zero will also be the point at which the real part of ω becomes zero, so the condition for marginal stability is just given by

$$\omega_o = 0$$

For the viscous dispersion relation, however, it is not obvious that the real and imaginary parts of ω both vanish at the point of marginal stability. That this is true can be shown by the application of the principle of the interchange of instabilities, as is done in Appendix A. Using the result derived there; namely,

$$\omega = 0$$

at the point of marginal stability, we find that the condition for marginal stability is again given by

$$\omega_o = 0$$

when the translational velocity V_o is set equal to zero, just as in the non-viscous case. The viscosity has no effect on the stability of the surface, although it will affect its rate of growth or decay.

2.4 The Thin Jet and the Thick Jet

Now let us make the approximation of a thin jet

$$k\Delta \ll 1 \; ; \quad m\Delta \ll 1$$

The expansions involving the viscosity terms must be taken to the second order in Δ since in the first order the result is the same as for the non-viscous jet. This might be expected, since the viscous dissipation is a volume effect, while the energy storage associated with the waves is at the surface. For a very thin jet, the surface to volume ratio is very high, and the viscosity accordingly has little effect. Making these substitutions, the dispersion relation, Eq. 2.46 becomes

$$y^2 - \frac{2\omega_o^2}{k\Delta} + \frac{iy\nu\Delta^2 k^4}{3} = 0 \qquad (2.48)$$

where use has been made of Eq. 2.23.

Now let us consider a thin jet with oscillations excited at a frequency ω, and look for the spatial behavior, that is, for k. We assume that the jet is infinite in the x_2 direction, and the wave propagates in the x_2 direction, so that

$$k_3 = 0$$

$$k = k_2$$

Now, Eq. 2.48 is quintic in k, so we will make the assumption that the jet velocity is much greater than the propagation velocity of the surface waves, or

$$k = \frac{\omega}{V_o} + \delta \qquad (2.49a)$$

$$\delta << \frac{\omega}{V_o} \qquad (2.49b)$$

Substituting this into Eq. 2.48, we find

$$0 = -\frac{2\omega_o^2}{\Delta} - \frac{i\nu\Delta^2 V_o}{3}\left(\frac{\omega}{V_o}\right)^5 \delta + \left[\omega V_o - \frac{5i\nu\Delta^2 V_o}{3}\left(\frac{\omega}{V_o}\right)^4\right] \delta^2 \qquad (2.50)$$

plus higher order terms in δ. All of the higher order terms are essentially lower order terms multiplied by $\delta V_o/\omega$ and may be neglected in the approximation $\delta << \omega/V_o$. From the definition of δ we see that a negative imaginary part corresponds to a growing wave, while a positive imaginary part corresponds to a decaying wave. Thus the viscosity tends to damp the wave. The wave will grow whenever $\omega_o^2 < 0$ and its growth rate is determined by Eq. 2.50. As expected, the stability criterion is identical to that of a non-viscous jet.

Defining the dimensionless parameters

$$E' = \frac{\varepsilon_o E_o^2}{\rho V_o^2} \qquad k' = \frac{kT}{\rho V_o^2} \tag{2.51a,b}$$

$$\omega^* = \frac{\omega T}{\rho V_o^3} \qquad b' = \frac{\rho V_o^2 b}{T} \tag{2.51c,d}$$

$$\nu' = \frac{\nu \rho V_o}{T} \qquad \Delta' = \frac{\rho V_o^2 \Delta}{T} \tag{2.51e,f}$$

$$\delta' = \frac{\delta T}{\rho V_o^2} \tag{2.51g}$$

the dispersion equation becomes

$$[1 - \frac{5i\nu'\Delta'^2\omega^{*3}}{3}]\delta^2 - \frac{i\nu'\Delta'^2\omega^{*4}}{3}\,\delta - \frac{2\omega^{*2}}{\Delta'} + \frac{2E'\omega^*}{\Delta'} \coth k'b' = 0 \tag{2.52}$$

The cutoff frequency is defined by

$$\delta' = 0 \tag{2.53a}$$

or

$$\omega' = E'\coth \omega'b' \tag{2.53b}$$

At the cutoff frequency, the dispersion relation takes the form

$$[1- \frac{5i\nu'\Delta'^2\omega^{*3}}{3}]\delta^2 - \frac{i\nu'\Delta'^2\omega^{*4}}{3}\delta' = 0 \tag{2.54}$$

One root, which describes the wave that is potentially unstable, is $\delta' = 0$. The other, which describes a wave which is always stable is

$$\delta' = \frac{i\nu'\Delta'^2\omega^{*4}}{3-5i\nu'\Delta'^2\omega^{*3}} \tag{2.55}$$

Then at the cutoff point of the growing wave, this stable wave has a propagation constant

$$k' = [\omega'-\frac{5\nu'^2\Delta'^4\omega^{*7}}{(9 + 25\nu'^2\Delta'^4\omega^{*6})}]+ \frac{3i\nu'\Delta'^2\omega^{*4}}{(9 + 25\nu'^2\Delta'^4\omega^{*6})} \tag{2.56}$$

This describes a damped wave with a phase velocity slightly faster than the equilibrium velocity of the fluid. In the limit of low viscosity, this becomes

$$k' = (\frac{\omega' - 5\nu'^2\Delta'^4\omega^{*7}}{9}) + i\ (\frac{\nu'\Delta'^2\omega^{*4}}{3}) \tag{2.57}$$

If the jet is very thick, $m\Delta >> 1$, $k\Delta >> 1$, and the dispersion relation reduces to

$$y^2(m^2 + k^2) + 2i\nu k^2(m-k)^2y - \omega_o^2(m^2 - k^2) = 0 \tag{2.58}$$

In the limit of low viscosity, $\nu k^2/\delta << 1$, this becomes

$$y^2 - 4i\nu k^2 y - \omega_o^2 = 0 \tag{2.59}$$

Again making the assumption

$$k = \frac{\omega}{V_o} + \delta \ , \quad \delta << \frac{\omega}{V_o} \tag{2.60}$$

The dispersion relation reduces to

$$\delta'^2[1-8i\nu'\omega'] - 4i\nu'\omega'^2\delta' - \omega'^3 + E'\omega'^2 \coth \omega'b = 0 \tag{2.61}$$

2.5 Experiments

Although the theory here presented is based on the assumption of a planar jet, the experimental work made use of a circular jet, due to the difficulty associated with the construction and operation of a planar jet. Although the two geometries are different, previous work on non-viscous fluid jets[1] indicates that the rate of growth of the unstable waves should be similar for the planar and the circular geometries.

The experimental apparatus for the study of the growing waves is sketched in Fig. 2.2. A jet of water leaves the reservoir tank at a constant velocity V_o through a circular nozzle. The jet then passes through the exciter section, which consists of two electrodes with applied potentials and spacings as described in Chapter III. However, spherical electrodes are used here instead of the flat plate electrodes described in Chapter III because it was found that a spherical electrode would eliminate the nulls in the frequency response curve.

After passing through the exciter, the grounded jet continues on between two metal plates at a high DC potential. The electric field at the surface of the jet due to this

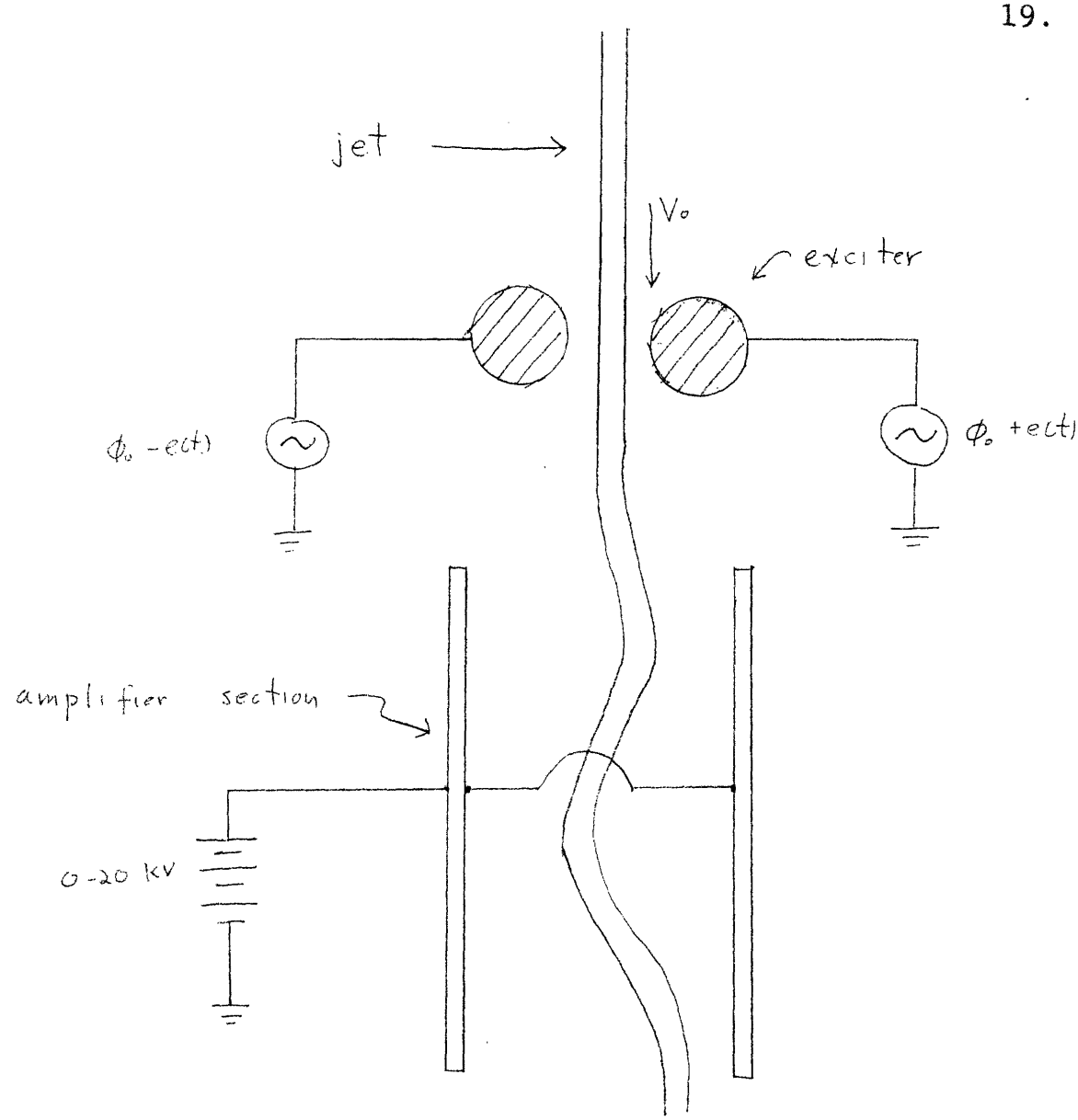

Figure 2.2 Experimental Setup for Growth Rate Measurements

applied voltage is large enough to cause the waves excited on the jet to grow. Photographs of the growing wave were taken, and from these photographs, measurements of the growth rate were made. The results are plotted in Fig. 2.3.

To evaluate the electric field at the surface of the jet theoretically would involve a laborious solution of Laplace's equation with the potential specified on the metal plates and the surface of the jet. The electric field can also be determined experimentally by measuring the cutoff frequency of the jet. Previous experimental work[1] indicates that the cutoff frequency can be predicted quite accurately in terms of the applied electric field for a circular jet. We have inverted this result to find the applied electric field from a measurement of the cutoff frequency.

For a jet of water of reasonable size, the theory indicates that the viscous damping of the surface waves is very slight, so slight that it may be neglected in the calculations with no noticeable error. For instance, for a jet of water (viscosity of 1 centipoise) 3 millimeters thick and moving at 3 meters per second, with a frequency of 300 cps. the complex part of k due to viscosity is of the order of -10^{-4} cm^{-1}, while that due to the electric field is on the order of 0.1 cm^{-1}. For the present experiment, the effect of the viscous damping is never greater than this, and so the effect of viscosity is not expected to be significant.

Since the jet is accelerating in a gravitational field, its velocity is not constant, and there is some doubt as to

Figure 2.3 δ vs ω' at $d = 0.33$ ($L = 30$ cm.)

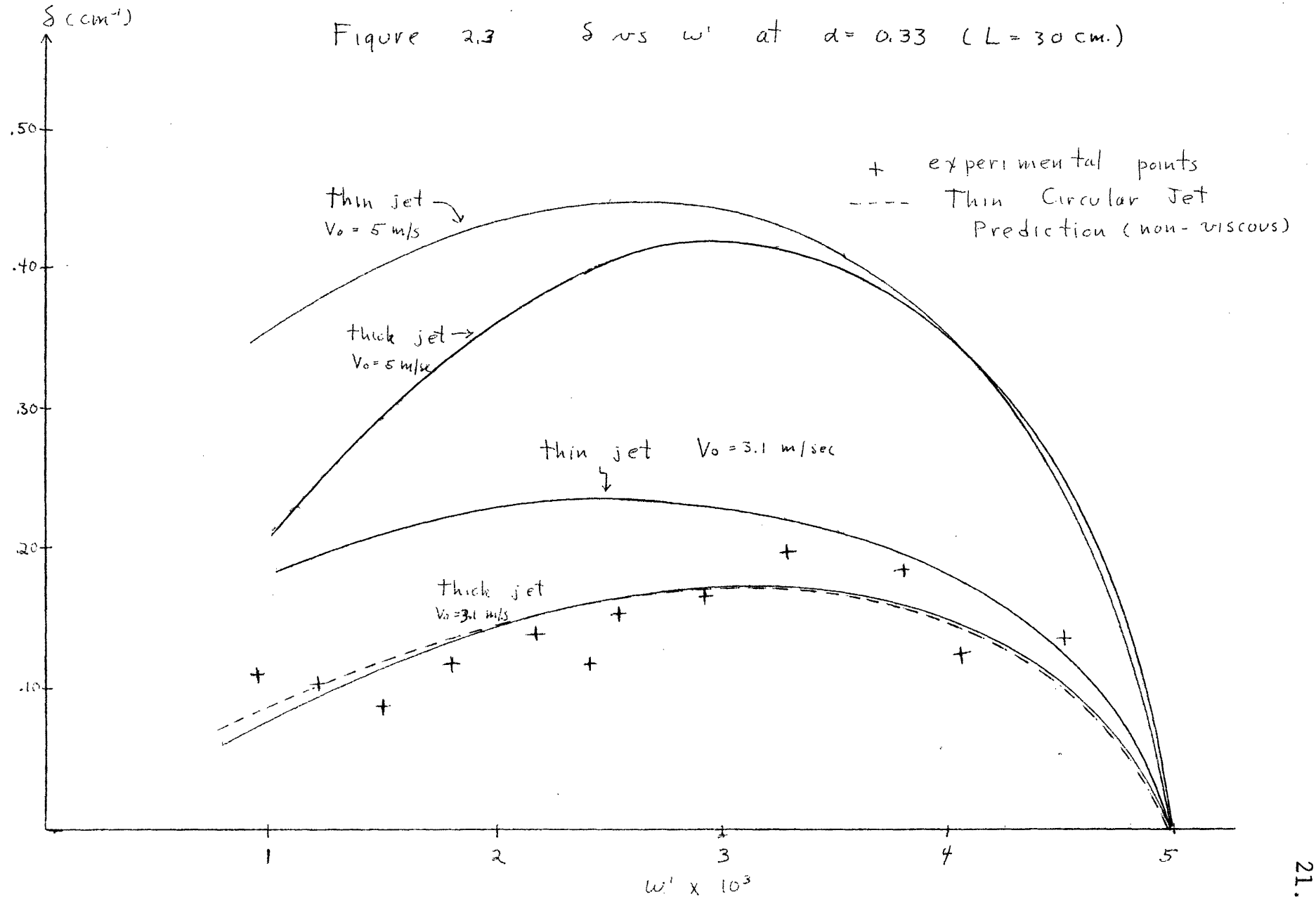

which value of velocity should be used in the equations. The growth rate has been calculated for the velocity at the exciter exit and for the velocity at the base of the amplifier section for a very thick and a very thin jet, and these results have been plotted along with the experimental results. The theoretical predictions for a thin non-viscous, circular jet, as derived by Melcher,[1] are also plotted in the same figure, for the two values of velocity. The two predictions are almost identical, and have been represented by a single dashed line.

From the figure it is apparent that the experimental results were predicted fairly accurately by the various theoretical models, with the thin, circular jet model giving perhaps the best results, not surprisingly. The results also indicate that the viscosity of the fluid plays a very small role in the growth rate under the experimental conditions.

CHAPTER III

Excitation of Waves on a Jet

3.0 Introduction

A practical problem which must be faced in conducting experiments of the type described in Chapter II is that of exciting the surface waves on the jet. In this work we excite the waves by means of an applied electric field.

As the grounded jet passes through the exciter section (Fig. 3.1), it is given an impulse by means of two electric fields of different strengths which are set up by the two exciter plates on either side of the jet. The voltage on the exciter plates is divided into a steady bias voltage and a sinusoidal signal voltage whose amplitude is less than the bias voltage. With this arrangement, it is possible to choose the voltages and plate to jet separations so that the deflection of the jet is linearly proportional to the signal voltage for a given frequency of excitation and distance along the jet.

3.1 The Theory of the Exciter

The exciter is modeled by two infinitely wide, perfectly conducting parallel plates of length ℓ on either side of the infinitely wide planar jet of perfectly conducting fluid (Fig. 3.1). The plates are separated from the grounded fluid by distances h_1 and h_2, and potentials $\phi_{o1} + e_1(t)$ and $\phi_{o2} - e_2(t)$ are applied to the plates.

Now, let us apply the impulse-momentum relation to a differential length of the jet, dx_1, which enters the exciter at time t_o and which is moving at a constant velocity V_o. The relation may be written

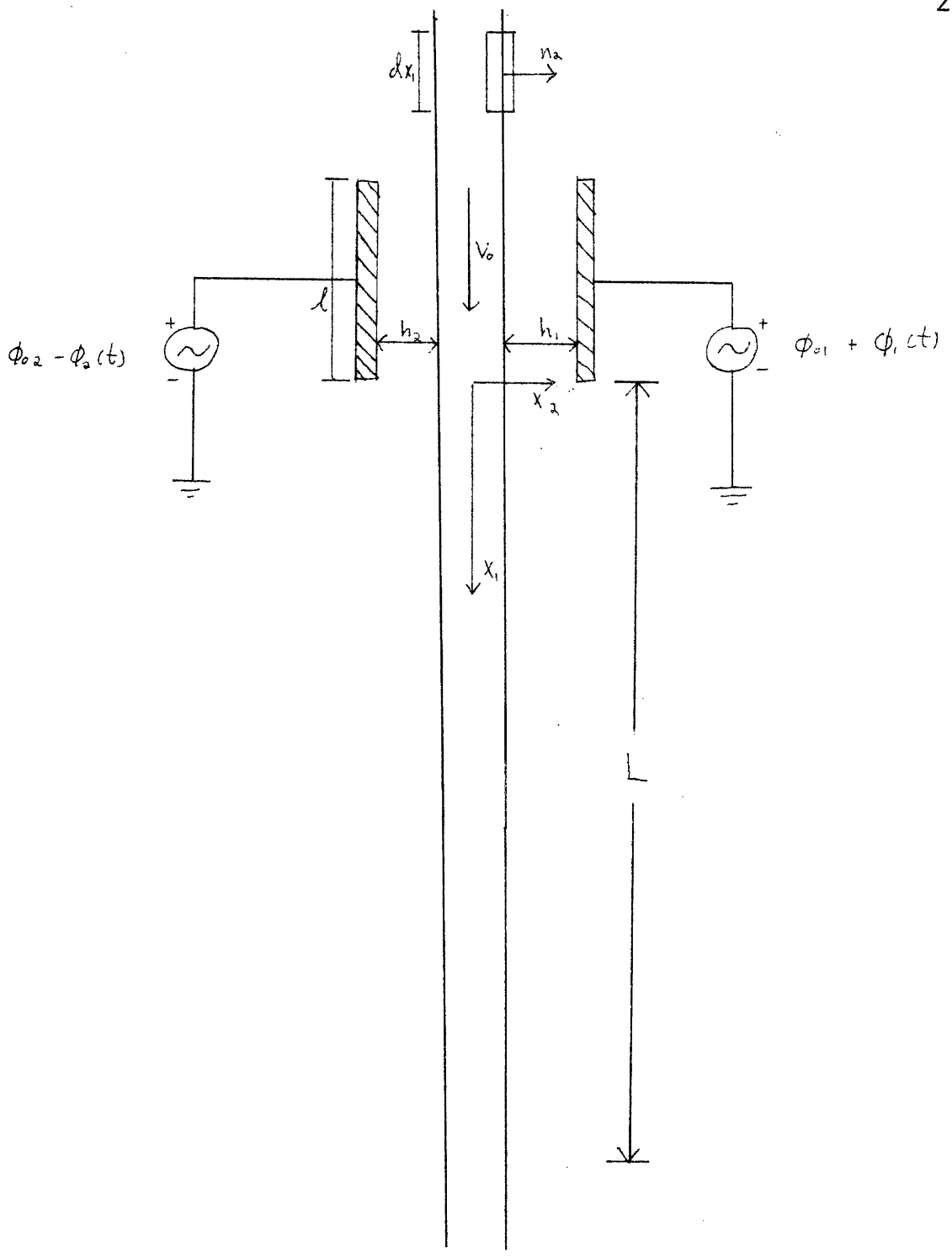

Figure 3.1

The Electric Field Exciter

$$dx_1 \int_o^{mv_2} d(mv_2) = dx_1 \int_{t_o}^{t_o + \ell/V_o} F(t)dt \qquad (3.1)$$

where m is the mass per unit length per unit width of the jet. The force on the differential length of the jet will be a function of time both through the variation of the field due to the applied signal voltage and to the motion of the jet. In the model we have chosen, a change in the electric field due to a change in geometry can occur only when the displacement of the jet in the exciter section becomes large enough to change the plate-to-jet separation appreciably. Since the experiments indicate that the jet suffers very little deflection in the exciter, we will neglect this effect, and assume that the variation of the force with time is due only to the variation in the signal voltage. This assumption also implies that surface tension has no effect on that portion of the jet inside the exciter.

The force per unit area on the surface of the jet can be found by means of the relation

$$F_i = \oint T_{ij} n_j da \qquad (3.2)$$

where T_{ij} represents the ij^{th} component of the Maxwell stress tensor at the surface of the jet, n_j is the outward normal to the j^{th} surface, and the integration is over a unit area. From this, the force per unit area is found to be

$$F_1 = F_3 = 0 \qquad (3.3a)$$
$$(3.3b)$$

$$F_2 = \frac{\varepsilon_o}{2}\left[\left(\frac{\phi_{o1}^2}{h_1^2} - \frac{\phi_{o2}^2}{h_2^2}\right) + 2\left(\frac{\phi_{o1}\phi_1}{h_1^2} + \frac{\phi_{o2}\phi_2}{h_2^2}\right) + \left(\frac{\phi_1^2}{h_1^2} - \frac{\phi_2^2}{h_2^2}\right)\right] \qquad (3.3c)$$

In order for there to be no net force on the jet when the bias is applied, we must satisfy the relation

$$\frac{\phi_{o1}}{h_1} = \frac{\phi_{o2}}{h_2} \tag{3.4}$$

and if the force is to be linearly proportional to the signal voltage, we must have

$$\frac{\phi_1}{h_1} = \frac{\phi_2}{h_2} \tag{3.5}$$

In this experiment,

$$\phi_1 = \phi_2 = \phi(t) \tag{3.5a}$$

$$h_1 = h_2 = h \tag{3.5b}$$

and

$$\phi_{o1} = \phi_{o2} = \phi_o \tag{3.5c}$$

If these conditions are fulfilled, the net force per unit area on the jet will be

$$F_2 = \frac{2\varepsilon_o \phi_o \phi(t)}{h^2} \tag{3.6}$$

If the signal voltage is

$$\phi(t) = e_o \cos \omega t$$

the force per unit area may be written

$$F(t) = \frac{2\varepsilon_o \phi_o e_o}{h^2} \cos \omega t \tag{3.7}$$

and the impulse-momentum relation becomes

$$\int_o^{mv_2} d(mv_2) = \int_{t_o}^{t_o + \ell/V_o} \frac{2\varepsilon_o \phi_o e_o}{h^2} \cos \omega t \, dt \tag{3.8}$$

This may be integrated to give

$$v_2 = \frac{2\varepsilon_o \phi_o e_o}{mh^2\omega}\left[\sin\left(\omega t_o + \frac{\omega \ell}{V_o}\right) - \sin \omega t_o\right] \tag{3.9}$$

By means of trigonometric identities, this may be rewritten as

$$v_2 = \frac{2\varepsilon_o \phi_o e_o}{mh^2\omega}\left[\left(\cos\frac{\omega\ell}{V_o} - 1\right)\sin\omega t_o + \left(\sin\frac{\omega\ell}{V_o}\right)\cos\omega t_o\right] \qquad (3.10)$$

Defining the dimensionless quantities

$$\omega' = \frac{\omega\ell}{V_o} \qquad (3.11)$$

$$v_2' = \frac{v_2 mh^2 V_o}{2\varepsilon_o e_o \phi_o \ell} \qquad (3.12)$$

the velocity response may be put in the form

$$v_2' = \frac{(\cos\omega'-1)}{\omega'}\sin\omega t_o + \frac{(\sin\omega')}{\omega'}\cos\omega t_o \qquad (3.13)$$

Here t_o, which represents the time of entrance of the differential length of the jet into the exciter, may be related to the real time at any point on the jet by an additive constant, so that Eq. 3.13 gives the velocity response of the jet to a sinusoidal input signal to within an additive phase constant. The magnitude of the response

$$|v_2'| = \frac{\sqrt{(\cos\omega'-1)^2 + (\sin\omega')^2}}{\omega'}$$

$$= \sqrt{2}\,\frac{\sqrt{1-\cos\omega'}}{\omega'} \qquad (3.14)$$

is plotted in Fig. 3.2. The response has nulls at

$$1-\cos\omega' = 0 \qquad (3.15)$$

or

$$\omega' = 2n\pi, \quad n \text{ integral} \qquad (3.16)$$

The maxima of the response may be found by setting the derivative of the response with respect to ω' equal to zero

$$\frac{\sin\omega'}{2\omega'\sqrt{1-\cos\omega'}} - \frac{\sqrt{1-\cos\omega'}}{\omega'^2} = 0 \qquad (3.17)$$

Figure 3.2

$\frac{\sqrt{2(1-\cos(\omega'))}}{\omega'}$ vs. ω'

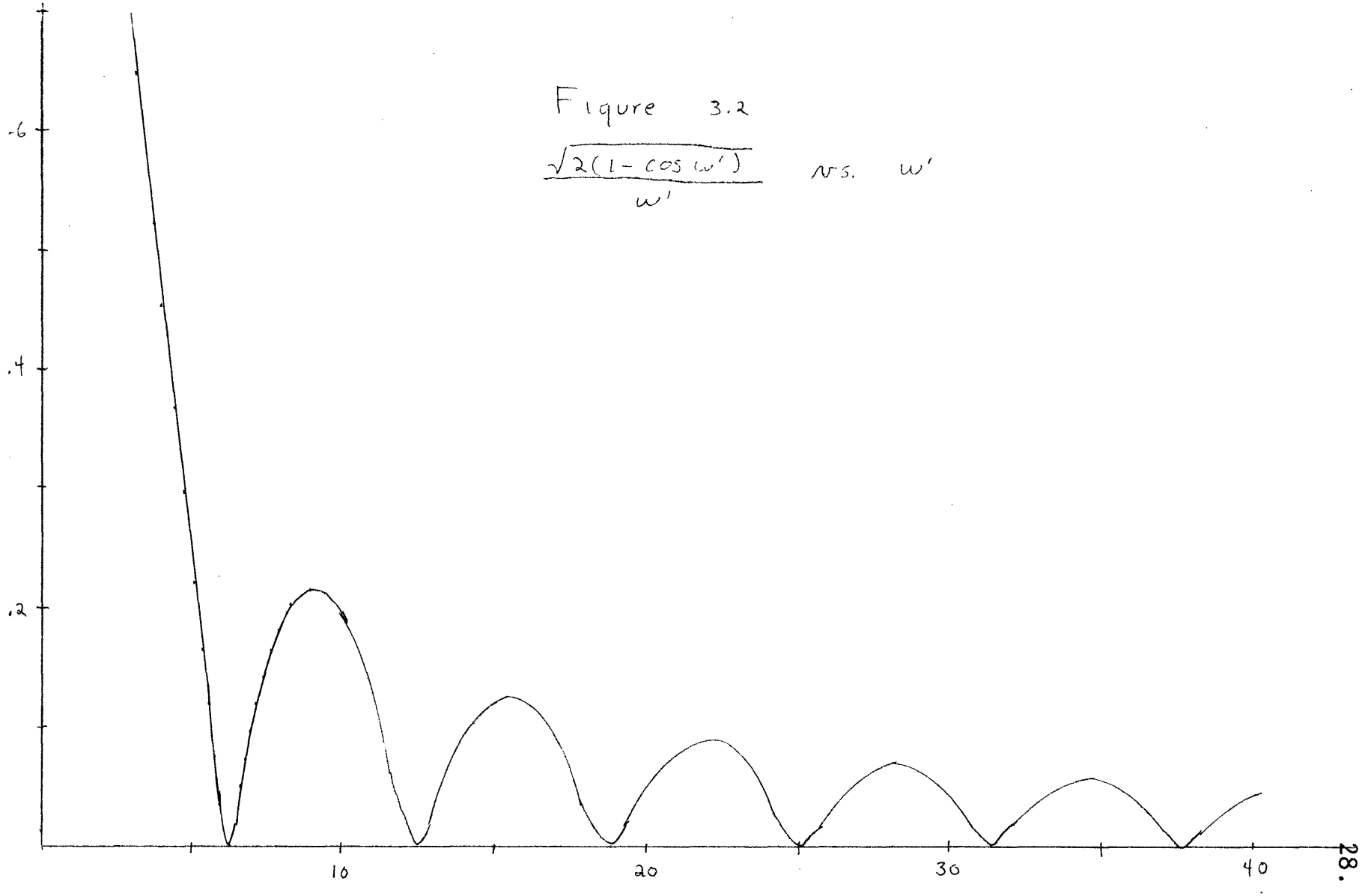

which yields

$$\omega' = 0 \tag{3.18}$$

and

$$\omega' \sin \omega' = 2(1-\cos \omega') \tag{3.19}$$

This yields two sets of solutions. One of them, $\omega' = 2n\pi$, gives us the minima of the function, which are identical with its nulls, and shows that the slope of the function at a null is zero. The other, which gives solutions which approach $(2n+1)\pi$ as n increases, represent the maxima of the function. The amplitude of the maxima fall off as ω^{-1} for high ω.

At low frequencies, $\omega' \rightarrow 0$, we find

$$2\,\frac{(1-\cos \omega')^{1/2}}{\omega'} \rightarrow 1 \tag{3.20}$$

so that

$$v_2' = 1 \tag{3.21}$$

This means that for low frequencies the velocity increment is given by

$$mv_2(t) = F(t)\Delta t \tag{3.21a}$$

where the force F(t) is essentially constant over the period of time Δt, a physically plausible result.

The phase angle is given by

$$\tan \theta_p = \frac{\cos \omega' - 1}{\sin \omega'} \tag{3.22}$$

to within an additive constant. This changes sign as we pass a null.

3.2 The Response of the Jet

Now, let us find the motion of the jet after it leaves the exciter. As we found in Chapter II, the deformation of the jet

can be described by means of waves with the dispersion relation

$$(\omega - kV_o)^2 = \omega_o^2 \coth \frac{k\Delta}{2} \tag{3.23}$$

neglecting viscosity, where

$$\omega_o^2 = \frac{Tk^3}{\rho} - \frac{\varepsilon_o E_o^2}{\rho} k^2 \coth kb \tag{3.23a}$$

We will now make the assumption that the jet is moving much faster than the propagation velocity of the surface waves, so that k may be written as

$$k = \frac{\omega}{V_o} + \delta \tag{3.24}$$

$$\delta << \frac{\omega}{V_o} \tag{3.24a}$$

Then we obtain

$$k_{\pm} = \frac{\omega}{V_o} \pm \delta \tag{3.25}$$

with

$$\delta = \left(\frac{\omega_o^2}{V_o^2} \coth \frac{k\Delta}{2}\right)^{1/2} \Bigg|_{k = \frac{\omega}{V_o}} \tag{3.25a}$$

The solution of the wave equation for the jet is

$$\xi(x_1,t) = \mathrm{Re}\left[\left(A_+ e^{+ik_+x_1} + A_- e^{ik_-x_1}\right) e^{-i\omega t}\right] \tag{3.26}$$

where $\xi(x_1,t)$ is the transverse displacement of the jet. The first boundary condition at $x_1 = 0$ is

$$\xi(0,t) = 0 \tag{3.27}$$

which requires that the jet leave the exciter with no net displacement. Using this condition we find

$$A_+ + A_- = 0 \tag{3.28}$$

The other boundary condition specifies the magnitude of the transverse jet velocity at the exciter exit.

$$\frac{d\xi}{dt}(0,t) = \frac{\partial \xi}{\partial t}(0,t) + V_o \frac{\partial \xi}{\partial x_1}(0,t) = v_2(0,t) \tag{3.29}$$

From this condition we obtain

$$A_+ = \frac{-i\, v_2(0)}{2V_o \delta} \tag{3.30}$$

Then the solution for $\xi(x_1,t)$ may be written

$$\hat{\xi}(x_1) = \frac{v_2(0)}{V_o \delta} (\sin \delta x_1) e^{i\omega x_1/V_o} \tag{3.31}$$

This shows that the displacement wave is the product of two sinusoids, one oscillating at the frequency determined by the excitation, and the other oscillating at a frequency which is the difference between the fast and the slow waves on the jet. The fast and the slow waves interact to give the effect of "beating" in space.

Now consider the special case in which the applied electric field is zero, and the jet is very thin, $k\Delta \to 0$. In these circumstances, we may write

$$\delta = \frac{\omega}{V_o^2}\sqrt{\frac{2T}{\rho\Delta}} \tag{3.32}$$

Then, defining the dimensionless quantities

$$\alpha = \frac{\omega}{V_o}\sqrt{\frac{2T}{\rho\Delta}}\,\frac{x_1}{\ell} \tag{3.33}$$

$$\xi' = \xi\left[\frac{2\varepsilon_o \phi_o e_o \ell^2}{mh^2 V_o}\sqrt{\frac{\rho\Delta}{2T}}\right]^{-1} \tag{3.34}$$

We may express the displacement response of the jet as a function of frequency and position as (combining Eqs. 3.14 and 3.30)

$$|\xi'| = \frac{\sin(\alpha\omega')\sqrt{2(1-\cos\omega')}}{\omega'^2} \tag{3.35}$$

Thus, the displacement response falls off as ω'^{-2}.
The function

$$\frac{\sqrt{1-\cos\omega'}}{\omega'^2}$$

is displayed in Fig. 3.3. This function gives the magnitude of the response at high frequencies, without the complicating effect of the term sin $\alpha\omega'$ which depends on the point at which the response is measured. Near $\omega = 0$ of course, this representation is not valid, since the term sin $\alpha\omega'$ approaches zero. This figure is plotted to the same scale as the velocity response of the exciter (Fig. 3.2), to show the strong effect on the response curve of the ω^{-2} dependence.

The maxima of the displacement response can be found by setting the derivative with respect to frequency of the response equal to zero.

$$\frac{\partial}{\partial\omega}\left(\frac{\sqrt{1-\cos\omega'}}{\omega'^2}\right) = 0$$

This gives the equation

$$\omega'\sin\omega' - 4(1-\cos\omega') = 0$$

The solutions of this equation for the maxima are again a series of frequencies which approach $(2n+1)\pi$ as n increases, but the frequencies of the maxima are always lower than the corresponding frequencies for the velocity response maxima.

Figure 3.3

$\frac{\sqrt{2(1-\cos\omega')}}{\omega'^2}$ vs. ω'

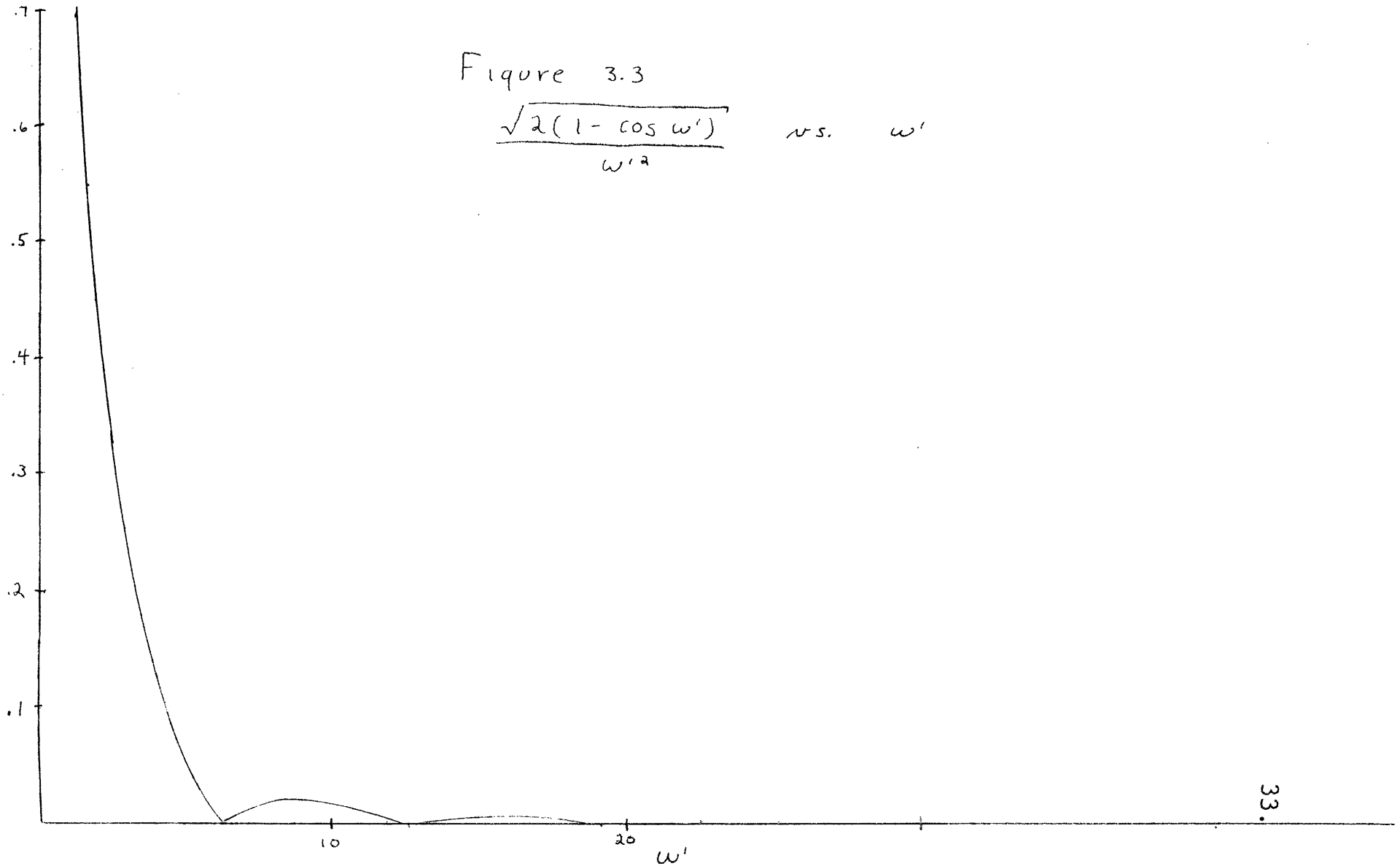

3.3 Experiments

Due to the difficulty of producing a planar jet and making accurate measurements on it, the experimental work was conducted on a circular jet. We must accordingly correct our model to take into account the change in the geometry of the system. The geometrical effect first affects the velocity response of the exciter by modifying the force of the electric field on the jet. To correct for this would require an exact solution of Laplace's equation for the situation in Fig. 3.4, a lengthy task. We will instead find an approximate value by using the minimum distance between the jet and the exciter plates for the quantity h. Continuing this approach, we will use the radius of the jet to calculate the mass per unit area instead of the thickness of a planar jet. These substitutions are permissible (for the exciter model used here) because the form of the exciter response does not depend on the shape of the jet, but only on the length of the jet in the exciter, and the distance from the exciter to the point of measurement.

As shown in Fig. 3.5, the jet of tap water issues from a long, tapered nozzle beneath a constant head of water maintained by an overflow system. The velocity of the jet at the nozzle is in the range 2-5 m/sec. depending on the head. After it leaves the nozzle, the jet passes between the exciter plates, where the electric field gives it an impulse. The jet then falls under in the earth's gravitational field for a known distance, and the amplitude of the disturbance on the jet is measured by means of a cathetometer.

Two types of measurements were made to test the theory. The first was a measurement of the position of the peaks and the nulls in the response curve. It was not possible to determine the amplitude for frequencies above the first null, since the

grounded jet flows into paper with velocity V_o

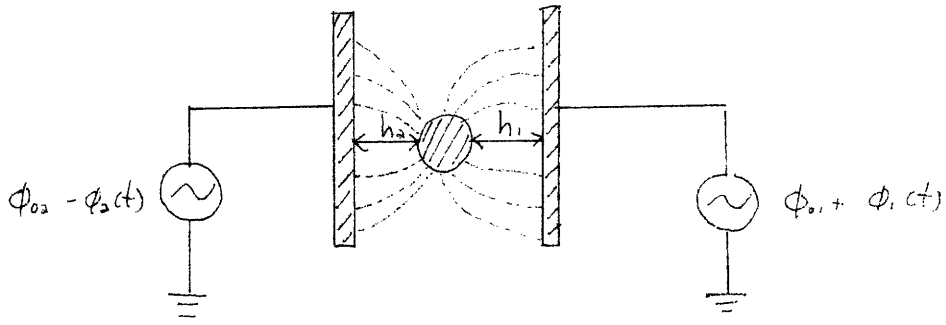

Figure 3.4 Electric Field in the Exciter

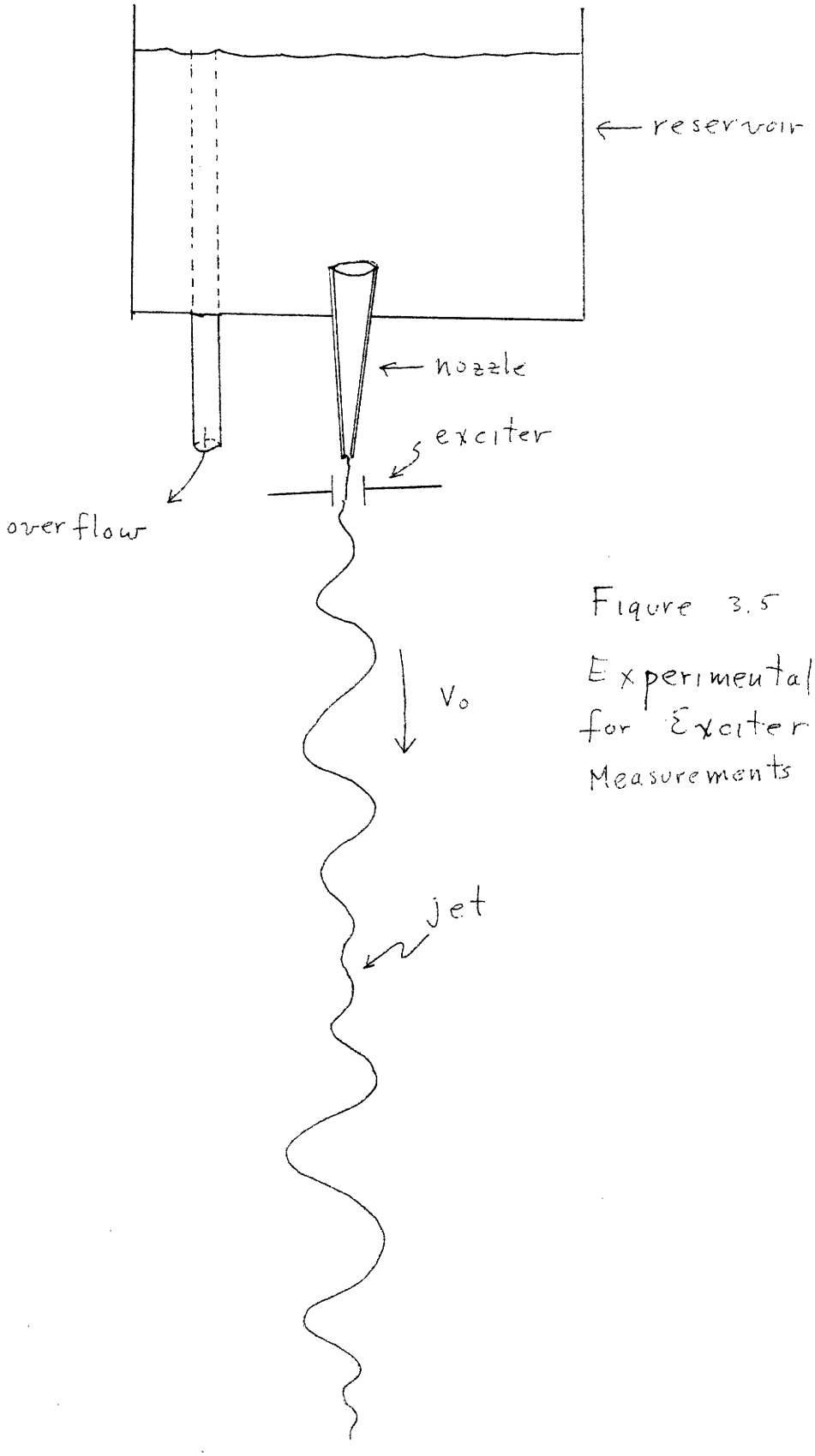

Figure 3.5

Experimental Setup for Exciter Measurements

displacement response of the jet at the higher frequencies was too small to measure reliably. In order to make the peaks and nulls in the response curve evident, an electric field large enough to cause growing waves was applied normal to the jet. (These growing waves were described in Chapter II.) The driving frequency was then adjusted until the jet appeared undisturbed and the frequency of the signal was measured with an electronic counter. The results of this measurement are plotted in Fig. 3.6. The scatter around the theoretically predicted position of the peaks and nulls may be partly attributed to the zero slope of the response curve at both the peaks and the nulls, so that both are relatively broad and ill-defined. It can be seen from the plot that the frequencies of the nulls are definitely lower than $(2n+1)\pi$ as would be expected from a simple sinusoidal response, offering a verification of the ω^{-2} dependence of the maximum response.

The displacement response of the exciter was also measured for frequencies below the first null with no applied electric field. Photographs of the jet were taken at various frequencies with the aid of a strobe lamp flashing at twice the frequency of the signal voltage. Measurements of the amplitude of the wave versus the distance along the jet were made from these photographs and the results plotted in Fig. 3.7. These plots indicate that the displacement response is sinusoidal in space, with the wavelength of the sinusoid decreasing as the frequency of the signal increases, as predicted by Eq. 3.35. From these plots the displacement response of the jet at any particular position may be found.

Figure 3.6 Frequency of Maxima and Nulls

Nulls Predicted at $\omega' = 2\pi, 4\pi, 6\pi$

Maxima Predicted at $\omega' = 8.55, 15.2, 21.6$

x - Experimental Point

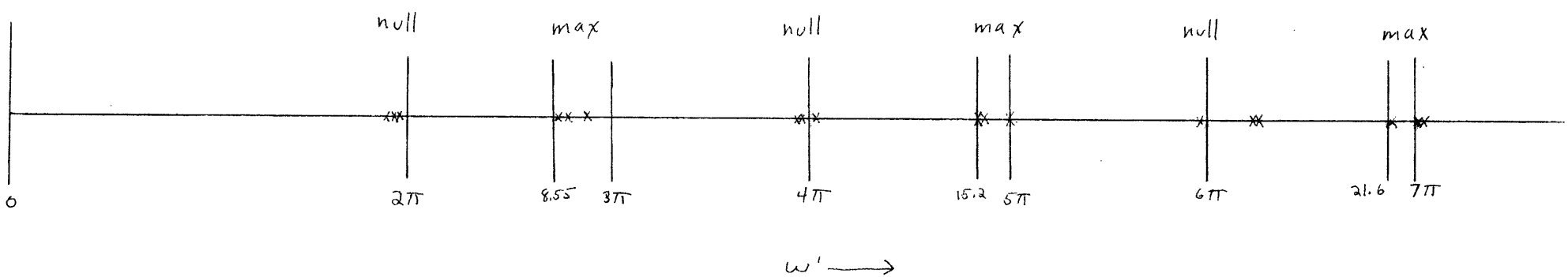

Figure 3.7 Wave Amplitude vs. Distance

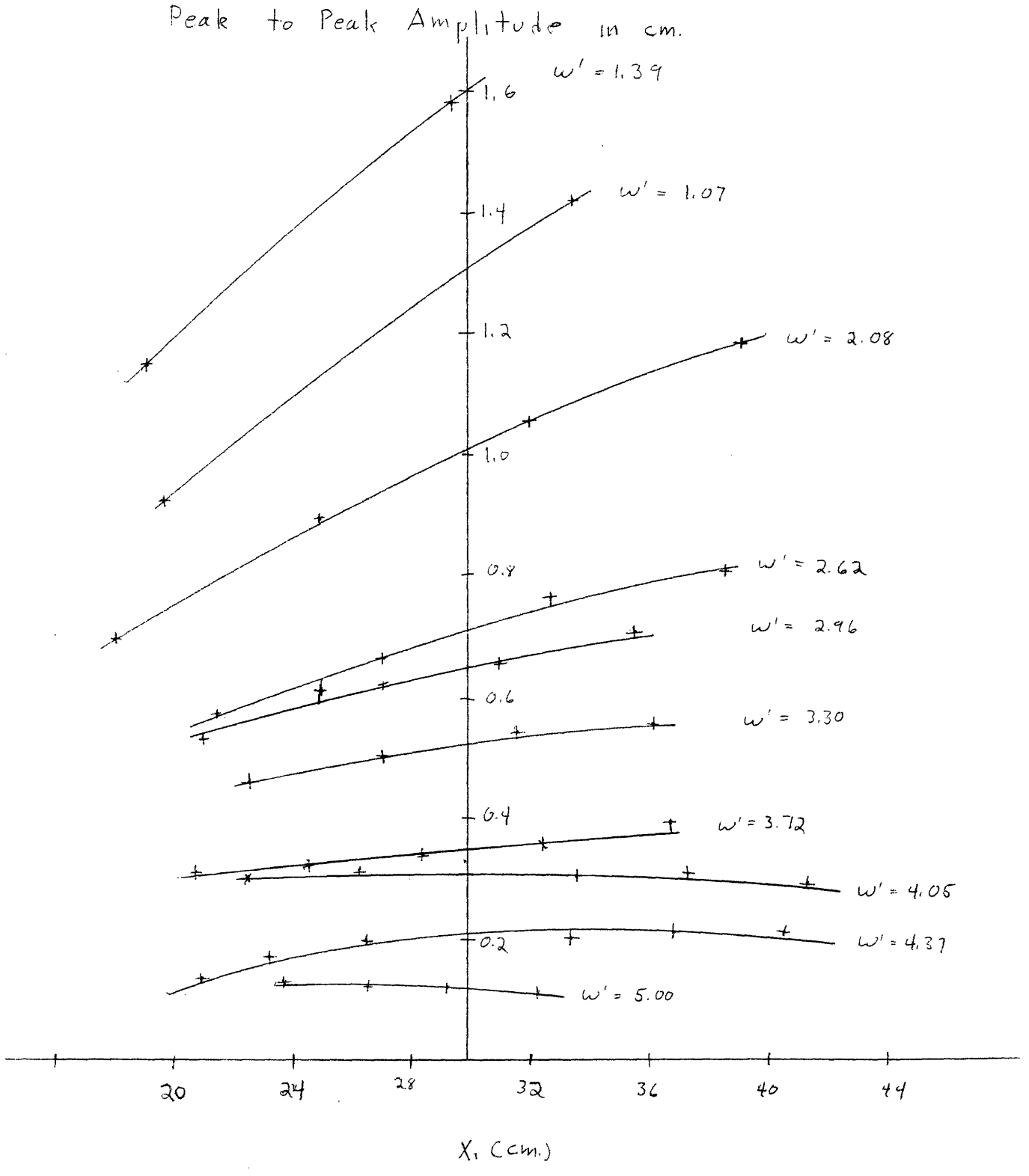

The values of the displacement were read from the graphs at a distance of 30 cm. from the exciter, and these displacement values were plotted versus frequency in Fig. 3.8. Now the jet used in the experiment was circular, and the jet postulated in the model was planar, so we would not expect a very close agreement between the absolute magnitude of the response curves for the two situations. The shape of the jet should not change the form of the response curve, however, since that is affected only by the length of the jet in the exciter and the distance from the exciter to the point of measurement. Accordingly, the theoretical response curve has been scaled to give a reasonable fit to the experimental results.

The theory also assumes that the velocity of the jet is constant, and for a jet falling in a gravitational field this is obviously untrue. As the jet falls, its velocity increases, and from the conservation of mass, its radius must decrease. Both of these effects will influence the parameter α which depends on both the velocity of the jet and the phase velocity of the surface waves. To give some idea as to the uncertainty in the predictions, the exciter displacement response curves corresponding to conditions at the exciter exit and at the point of measurement were both plotted along with the experimental results. It can be seen that the response at the higher frequencies is not affected by the difference in the values of α, but that at lower frequencies there is a fairly large difference between the two theoretical predictions, indicating that the response is more sensitive to slight perturbations in this range. It should be noticed that the experimental points also show more scatter in this frequency range, but that the

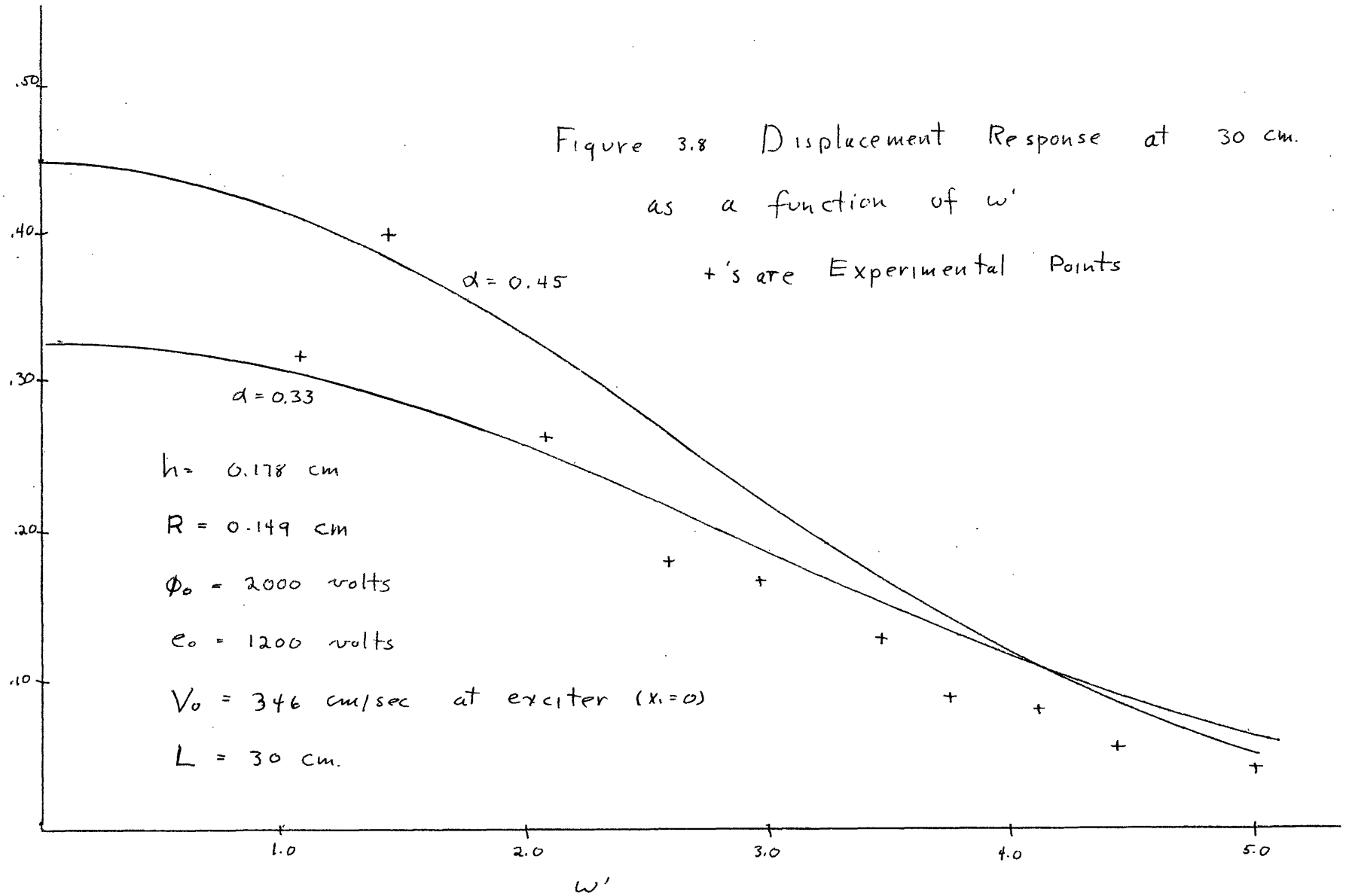

Figure 3.8 Displacement Response at 30 cm. as a function of ω'

+'s are Experimental Points

points are still more or less contained between the two extremes of the theory.

From the experimental points, it appears that the response falls off somewhat faster than expected at high frequencies. This may be due to the effect of fringing fields at the edges of the exciter plates, since the wavelength of the disturbance is not much larger than the separation of the two plates at these frequencies. Also, it was noticed in the course of the experiment that when the plates were separated about five times as far as in this measurement, the response fell off approximately twice as fast at the higher frequencies.

A rough estimate of the magnitude of the displacement response was made for a frequency of 15 cps at a distance of 30 cm from the exciter from the planar jet formula, Eq. 4.33. This predicted a peak-to-peak displacement of approximately 1.1 cm while the measured peak-to-peak displacement of the jet for these conditions was around 1.4 to 1.6 cm, a fairly good agreement considering all the approximations made in going from the planar geometry to the circular.

The equation obtained for the displacement response, Eq. 3.33, predicts nulls in the response at distances from the exciter determined from the equation

$$\sin\left(\frac{\omega L}{V_o^2}\sqrt{\frac{2T}{\rho\Delta}}\right) = 0$$

or

$$L = \frac{n\pi V_o^2}{\omega}\sqrt{\frac{\rho\Delta}{2T}}, \qquad n \text{ integral}$$

Here again, the precise distance at which the null should be observed is obscured by the acceleration of the jet. The

observation of this null is further complicated by the inherent instability of a circular jet, which tends to break up into little droplets,[5] thus violating our continuum approach. In spite of these difficulties, the null was actually observed for a frequency of 75 cps at a distance of 45 cm from the exciter. The velocity of the jet at the exciter was 300 cm/sec. This observed distance is bracketed by the predictions made on the bases of conditions at the exciter and at the point of measurement, 27 cm and 93 cm.

These experimental data offer evidence that the model used in this analysis describes the electric field EHD exciter.

APPENDIX A

A Criterion for the Onset of Instability

The proof that the onset of instability is determined by the condition

$$\omega = 0$$

is given by Chandrasekhar[4] for a disturbance on the surface of a fluid. In his analysis he considers the effect of gravity, surface tension, and viscosity. To show that the same condition applies in EHD systems, we will generalize his derivation to include the effect of an electric pressure at the surface of the liquid. The effect of gravity will be neglected. The equations of the system may be written (cf. Ref. 4, Ch. X, Eqs. 70, 15, 16, 17)

$$Dp = i\omega\rho v_1 + \mu(D^2 - k^2)v_1 + 2(Dv_1)(D\mu) + [k^2T - k\varepsilon E_o^2 \coth kb] \sum_s \frac{v_1(\xi_s)}{i\omega} \delta(x_1 - \xi_s) \tag{A.1a}$$

$$ik_2p = i\omega\rho v_2 + \mu(D^2 - k^2)v_2 + (D\mu)(ik_2v_1 + Dv_2) \tag{A.1b}$$

$$ik_3p = i\omega\rho v_3 + \mu(D^2 - k^2)v_3 + (D\mu)(ik_3v_1 + Dv_3) \tag{A.1c}$$

$$Dv_1 + ik_2v_2 + ik_3v_3 = 0 \tag{A.2}$$

where we have allowed the viscosity to be functions of space. These equations merely express the force balance on the fluid and the continuity of the fluid, where the surface tension and electric pressure have been considered as forces which act only at the surface. This is expressed by the summation sign, which sums over the various interfaces in the system, and the Dirac delta function, which is non-zero only at the s^{th} interface, $x_1 = \xi_s$. We have also assumed that all quantities may be expressed as waves propagating in the x_2x_3 plane.

Multiplying Eq. A.1b by k_2 and Eq. A.1c by k_3, adding and using Eq. A.2, we get

$$k^2 p = i\omega\rho Dv_1 + \mu(D^2 - k^2)(Dv_1) + (D\mu)(D^2 + k^2)v_1 \qquad (A.3)$$

Eliminating p between this equation and Eq. A.1a we find

$$D\left\{[\rho + \frac{\mu}{i\omega}(D^2 - k^2)]Dv_1 + \frac{1}{i\omega}(D\mu)(D^2 + k^2)v_1\right\} =$$

$$k^2\left\{[\rho + \frac{\mu}{i\omega}(D^2 + k^2)]v_1 + \frac{2}{i\omega}(D\mu)(Dv_1)\right.$$

$$\left. + \frac{1}{\omega^2}[-\sum_s(k^2T - \varepsilon E_o^2 k \coth kb)\delta(x_1 - \xi_s)]v_1(\xi_s)\right\} \qquad (A.4)$$

We will now assume two solutions for v_1

$$v_1 = u_i$$

$$v_1 = u_j$$

and the corresponding values of ω

$$\omega = \omega_i$$

$$\omega = \omega_j$$

Writing Eq. A.1a for u_i, multiplying by u_j and integrating from $-\infty$ to $+\infty$ we obtain

$$\int_{-\infty}^{\infty} u_j Dp_i dx_1 = \int_{-\infty}^{\infty} (i\omega\rho - k^2\mu)\, u_i u_j dx_1$$

$$+ \int_{-\infty}^{\infty} [u_j \mu D^2 u_i + 2u_j (D\mu)(Du_i)]dx_1$$

$$+ \frac{1}{i\omega_i}\int_{-\infty}^{\infty} \sum_s (k^2T - \varepsilon E_o^2 k \coth kb)u_i(\xi_s)u_j(\xi_s)$$

For the remainder of the section, we will omit the limits on the integrals for convenience. Since the disturbance of the fluid is

localized to the jet we may take as a boundary condition the restriction that both the velocity and its space derivative approach zero far from the jet.

Integrating the left-hand side of Eq. A.5 by parts, we get

$$\int u_j Dp_i dx_1 = -\int p_i Du_j dx_1 \tag{A.6}$$

Now substituting the value of p from Eq. A.3,

$$-\int p_i Du_j dx_1 = -\int \left(\frac{i\omega_i \rho}{k^2} - \mu\right)(Du_i)(Du_j)dx_1$$

$$-\int (D\mu)u_i(Du_j)dx_1 - \frac{1}{k^2}\int D(\mu D^2 u_i)(Du_j)dx_1 \tag{A.7}$$

Integrating the last term by parts

$$\int Du_j D(\mu D^2 u_i)dx_1 = -\int \mu D^2 u_i D^2 u_j dx_1 \tag{A.8}$$

Eq. A.7 becomes

$$-\int p_i Du_j dx_1 = -\int \left(\frac{i\omega_i \rho}{k^2} - \mu\right)(Du_i)(Du_j)dx_1$$

$$-\int (D\mu)u_i(Du_j)dx_1 + \frac{1}{k^2}\int \mu(D^2 u_i)(D^2 u_j)dx_1 \tag{A.9}$$

combining this with Eq. A.5, we find

$$i\omega_i \int \rho[u_i u_j + \frac{1}{k^2}(Du_i)(Du_j)]dx_1$$

$$+ \frac{1}{i\omega_i}\sum_s (k^2 T - \varepsilon E_o^2 k \coth kb)u_i(\xi_s)u_j(\xi_s) =$$

$$\int \mu[k^2 u_i u_j + (Du_i)(Du_j) + \frac{1}{k^2}(D^2 u_i)(D^2 u_j)]dx_1 -$$

$$-\int \left[u_j[\mu D^2 u_i + 2(D\mu)(Du_i)] + u_i(D\mu)(Du_j)\right]dx_1 \tag{A.10}$$

The last term is equal to

$$-\int \left\{u_j D(\mu Du_i) + (D\mu)D(u_i u_j)\right\}dx_1 = \int \left\{\mu(Du_i)(Du_j) + (D^2\mu)u_i u_j\right\}dx_1 \tag{A.11}$$

Multiplying by ω_i, we now have the equation

$$i\omega_i^2 \int \rho \left\{ u_i u_j + \frac{1}{k^2}(Du_i)(Du_j) \right\} dx_1 - i\Sigma_s [k^2 T - \varepsilon E_o^2 k \coth kb] u_i(\xi_s) u_j(\xi_s)$$

$$= \omega_i \int (D^2\mu) u_i u_j dx_1 + \omega_i \int \mu [k^2 u_i u_j + 2(Du_i)(Du_j) + \frac{1}{k^2}(D^2 u_i)(D^2 u_j)] dx_1 \tag{A.12}$$

If we now interchange the indices i and j and subtract we get the equation

$$-(\omega_i^2 - \omega_j^2)\left[\int \rho \left\{ u_i u_j + \frac{1}{k^2}(Du_i)(Du_j) \right\} dx_1\right] = i(\omega_i - \omega_j)$$

$$\left[\int (D^2\mu) u_i u_j dx_1 + \int \mu [k^2 u_i u_j + 2(Du_i)(Du_j) + \frac{1}{k^2}(D^2 u_i)(D^2 u_j) dx_1\right], \quad (\omega_i \neq \omega_j) \tag{A.13}$$

If we take ω_i and ω_j to be complex conjugates, we have, dividing by $i\omega_i - i\omega_j$,

$$2\mathrm{Re}(i\omega) \int \rho \left\{ |u|^2 + \frac{1}{k^2} |Du|^2 \right\} dx = \int (D^2\mu) |u|^2 dx_1$$

$$+ \int \mu \left(|u|^2 k^2 + 2|Du|^2 + \frac{1}{k^2} |D^2 u|^2 \right) dx_1 \tag{A.14}$$

The integrand of the integral

$$\int (D^2\mu) |u|^2 dx_1$$

is non-zero only at the interface, since the fluid properties, including the viscosity, are constant except at the interface. At the interface, however, the viscosity is a step function, so that its second derivative is a doublet. The integral may now be written

$$\int_{-\infty}^{\infty} (D^2\mu) |u|^2 dx \propto \mu \left(\frac{d}{dx_1} |u|^2 \Big|_{\Delta/2+\xi} - \frac{d}{dx_1} |u|^2 \Big|_{-\Delta/2+\xi} \right) \tag{A.15}$$

For the motion we are considering, the upper and the lower surfaces of the jet move together, so that the term in parentheses vanishes by symmetry, and the integral accordingly equals zero.

All the remaining terms in the equation are positive definite, and we have the result that if $\omega_i \neq \omega_j$, the real part of $i\omega$ is positive, corresponding to a stable decaying disturbance. Conversely, if the real part of $i\omega$ is negative, corresponding to a growing disturbance, then $\omega_i = \omega_j$ and the growth is pure exponential, with no sinusoidal components. Since all growing disturbances are characterized by a real value of $i\omega$, we can find the state of marginal stability by letting $i\omega$ approach 0 through positive values or equivalently setting

$$\omega = 0 \tag{A.16}$$

This means that the marginal state is stationary and not characterized by a constant amplitude sinusoidal motion.

APPENDIX B

Bibliography

1. Melcher, J.R., Field Coupled Surface Waves: A Comparative Study of Surface Coupled Electrohydrodynamic and Magnetohydrodynamic Systems, MIT Press, Cambridge, Mass., 1963.

2. Hoppie, L.O., "The Electrohydrodynamic Traveling-Wave Amplifier: An Application of Low Conductivity Plasma," S.B. Thesis, Dept. of Elec. Eng., MIT, May, 1962.

3. Lyon, J.F., "The Electrohydrodynamic Kelvin-Helmholtz Instability," S.M. Thesis, Dept. of Elec. Eng., MIT, Sept., 1962.

4. Chandrasekhar, S., Hydrodynamic and Hydromagnetic Stability, Oxford at the Clarendon Press, London, 1961.

5. Lamb, H., Hydrodynamics, Dover Publications, New York, 1945.